Salt-Induced DNA-Histone Complexation

K.-K. Kunze and R. R. Netz
Max Planck Institute of Colloids and Interfaces, 14424 Potsdam, Germany
(Received 3 May 2000)

We study numerically the binding of one semiflexible charged polymer onto an oppositely charged sphere. Using parameters appropriate for DNA-histone complexes, we find complete wrapping for intermediate salt concentrations only, in agreement with experiments. For high salt concentrations, a strongly discontinuous dewrapping occurs. For low salt concentrations, we find multiple conformational transitions, leading to an extended DNA configuration. The wrapped states are characterized by spontaneously broken rotational and mirror symmetries, giving rise to four distinct structures.

PACS numbers: 87.15.–v, 61.25.Hq, 82.70.Dd

The interaction of polyelectrolytes (PE) with oppositely charged spheres is a recurring theme in a multitude of commercial and biological systems. Examples include synthetic PE adsorbing on colloidal particles [1], micelles [2], proteins [3], and DNA binding to latex particles [4], dendrimers [5], and proteins [6]. These examples differ in the size and charge of the spherical particles and the stiffness and linear charge density of the PE. Applications of synthetic PE-particle complexes include the control of dispersion stabilization, flocculation, and precipitation, while charged biopolymer-particle complexes are used for the immobilization of enzymes and purification of proteins.

Theoretically, PE-sphere complexation has been studied with simulations [7,8], showing that wrapping takes place when the PE linear charge density and sphere charge are high enough. Mean-field theories were used to characterize the bound state for the case of flexible polymers [8–11]. For stiff polymers, simplified models for DNA-protein binding described a wrapping transition as a function of a few phenomenological parameters [12,13], while a recent scaling theory characterized the wrapped state as a function of the physical parameters of the system [14].

In this paper, we numerically investigate a simplified model for the interaction between a charged sphere, characterized by its radius and charge, and an oppositely charged, semiflexible PE, characterized by its bending stiffness and linear charge density. We specifically treat the case of complexation of DNA with histone proteins and systematically investigate the influence of varying salt concentration and sphere charge on the equilibrium complexation behavior. Nature uses the binding of DNA, a negatively charged stiff biopolymer, to the positively charged histone proteins to compact and store the approximately 1 meter of human DNA in a nucleus of perhaps 10 μm. The compact structure contains a repetitive structure whose basic elements are the nucleosomal particles, consisting of DNA wrapped in about 2 turns around the histone protein. The stability of these nucleosomal particles is of importance for the biological activity of DNA and has been investigated in detail. A particularly useful line of experiments investigates the effects of salt on a solution of histones, each with exactly 146 base pairs of DNA wrapped around. Using a variety of different experimental techniques, the main characteristics of the complexation behavior are the following [15]: For salt concentrations close to the physiological value of about $100mM$, the DNA is tightly wrapped around the histone. For large salt concentration of about $750mM$ the DNA is released from the complex (while for even larger salt concentrations the histone protein disintegrates into its eight parts). For small salt concentration below around $2mM$, the DNA takes an extended form, which is indicative of a partial dewrapping of the DNA from the histone [16,17]. This low-salt transition is believed to occur in two steps [18]. Since salt modulates electrostatic interactions, this suggests that the binding of this complex is predominantly of electrostatic character. Indeed, our simple model, which neglects all nonelectrostatic interactions, is able to reproduce the experimental sequence of complexed states upon variation of the salt concentration and explains them in terms of spontaneously broken rotational and mirror symmetries, giving rise to four distinct wrapped states.

In our model, the DNA is described by a semiflexible polymer of length $L = 50$ nm (corresponding roughly to 146 base pairs of length 0.34 nm each) with a bare mechanical persistence length of $l_P = 30$ nm [19]. The histone protein is approximated as a rigid sphere of radius $R = 5$ nm which exhibits no structural changes. For the interaction between the charges on the DNA and the sphere we use Debye-Hückel potentials. For a given DNA configuration $\mathbf{r}(s)$ the free energy reads

$$\frac{\mathcal{F}}{k_B T} = \frac{l_P}{2}\int_0^L ds\, \ddot{\mathbf{r}}^2(s) - \frac{l_B Z\tau}{1+\kappa R}\int_0^L ds\, \frac{e^{-\kappa(|\mathbf{r}(s)|-R)}}{|\mathbf{r}(s)|} + l_B\tau^2\int_0^L ds\int_s^L ds'\, \frac{e^{-\kappa|\mathbf{r}(s)-\mathbf{r}(s')|}}{|\mathbf{r}(s)-\mathbf{r}(s')|}. \quad (1)$$

The first term describes the bending energy, the second term describes the electrostatic attraction between the sphere (of charge Z in units of the elementary charge) and the DNA (of linear charge density τ), and the third term describes the electrostatic repulsion between different DNA segments. The Bjerrum length $l_B = e^2/4\pi\varepsilon\varepsilon_0 k_B T$

measures the distance at which two elementary charges interact with thermal energy k_BT. At room temperature in water $l_B = 0.7$ nm. κ is the inverse Debye-Hückel screening length, which is given by $\kappa = \sqrt{8\pi l_B c}$ in a monovalent salt solution of concentration c. We implicitly add a hard-core interaction between the sphere and DNA segments and keep the tangent vectors normalized according to $|\dot{\mathbf{r}}(s)| = 1$. We fix the linear DNA charge density at a value $\tau = 2/0.34$ nm corresponding to the maximal possible degree of dissociation of two charges per base pair and thus neglect nonlinear effects connected with counterion condensation on either DNA or sphere. The main reason for doing this is that no closed-form expression for the nonlinear potential of a sphere or a cylinder in a salt solution is available. The sometimes used approximation of charge renormalization has been shown to be equally flawed for high salt concentration and large cylinders [20]; we therefore decided to use regular Debye-Hückel potentials. Also, we approximate the histone by a sphere, the DNA by a line, smear out the charges on the histone and the DNA, and neglect DNA twist degrees of freedom and effects due to different DNA base sequences. This is, at best, a caricature of reality. However, the basic features of the complexation behavior are quite striking and robust, and to a large extent independent of details.

Since the persistence length of the chain is, including electrostatic stiffening effects, at least 30 nm and thus larger than the sphere diameter, one can to a good approximation neglect thermal fluctuations of the chain and thus also undulation forces [14]. We therefore perform a systematic ground state analysis of the problem, looking for the DNA configuration which minimizes the free energy Eq. (1). In order to perform the numerical analysis, we discretize the DNA configuration with up to 400 discretization points. We explicitly checked that discretization effects are negligible so our results correspond to the continuum limit.

In Fig. 1 we show a series of DNA configurations obtained for a fixed sphere charge $Z = 40$ and for inverse screening lengths ranging from $\kappa = 0$ nm^{-1} to 10.6 nm^{-1}.

In Fig. 1(a) the pure Coulomb case with no added salt is shown. The DNA shows two-fold rotational symmetry around the z axis and mirror symmetry. The pronounced Coulomb repulsion between DNA segments bends the two arms away from the sphere. This behavior is characteristic for all situations when the screening length is larger or roughly similar to the sphere diameter, i.e., for $2R < \kappa^{-1}$. At a slightly elevated salt concentration, Fig. 1(b), the rotational symmetry is discontinuously broken. The fully symmetric configuration, to the left, coexists with a configuration where one arm is wrapped around the sphere while the other extends straight away from the sphere, to the right. This configuration has been observed previously in a numerical simulation [8]. From the top and bottom views of the complex it can be seen that mirror symmetry is preserved. At $\kappa = 0.13$ nm^{-1} this mirror symmetry is continuously broken. Figure 1(c) shows the planar configuration right at the transition, Fig. 1(d) shows the nonplanar configuration at a slightly elevated salt concentration $\kappa = 0.14$ nm^{-1}. It is seen that the wrapped DNA arm moves out of the plane of symmetry. In the salt concentration range between $\kappa = 0.13$ nm^{-1} and $\kappa = 0.42$ nm^{-1} the free arm of the DNA is continuously drawn towards the sphere, but no symmetry change takes place. At $\kappa = 0.42$ nm^{-1} the rotational symmetry is restored in a weakly discontinuous transition. The two coexisting structures shown in Fig. 1(e) are rather similar and correspond to a more or less fully wrapped state. In the salt concentration range between $\kappa = 0.42$ nm^{-1} and $\kappa = 10.6$ nm^{-1} the DNA is tightly wrapped around the sphere. At $\kappa = 10.6$ nm^{-1} a strongly discontinuous transition occurs in which the DNA completely unwraps from the sphere. Figure 1(f) shows the two coexisting states. The unwrapped state at high salt concentration is markedly different from the state at low salt concentration shown in Fig. 1(a): There is only one short region of nonzero bending of the DNA connecting two basically straight arms.

As the DNA configurations demonstrate, the DNA-sphere complex can be characterized by two distinct symmetries, which can be spontaneously broken in the wrapped state. The first symmetry is quantified by the order parameter $\eta = [\boldsymbol{r}(0)^2 - \boldsymbol{r}(L)^2]/L^2$ which measures the amount to which the twofold rotational symmetry around an axis through the polymer center is broken. The second order parameter is the torsion of the polymer, $\sigma = L^{-1}\int_0^L ds\, \dot{\mathbf{m}}(s) \cdot \dot{\mathbf{r}}(s) \times \mathbf{m}(s)$ where $\mathbf{m}(s) = \ddot{\mathbf{r}}(s)/|\ddot{\mathbf{r}}|$ is the normalized bending vector. This order parameter measures whether (and to what extent) the mirror symmetry of the polymer is broken. One of the main results of this paper is that the two symmetries are in fact broken independently from each other: We find a total of four different phases, corresponding to all different combinations of symmetry breakings. This is demonstrated clearly in Fig. 2, where we plot the 2 order parameters at fixed sphere charge $Z = 40$ as a function of the inverse screening length κ, the same parameters for which we showed configurations in Fig. 1.

The complete phase diagram is presented in Fig. 3. In Fig. 3(a) we show only the transition from the rotationally symmetric, mirror-asymmetric state ($\eta = 0, \sigma \neq 0$) to the totally asymmetric state ($\eta \neq 0, \sigma \neq 0$). In the absence of salt, for $\kappa = 0$, this transition occurs at $Z = 136.5$. In agreement with experiments, complexation is most pronounced at intermediate salt concentrations. For low salt, the strong DNA-DNA repulsion prevents complexation, for high salt the weakening of the DNA-sphere attraction induces dewrapping. The minimal sphere charge to wrap the DNA, $Z \approx 10$, is obtained for $\kappa^{-1} \approx 1$ nm, corresponding to physiological conditions. Since the total charge on the DNA is about 300, the

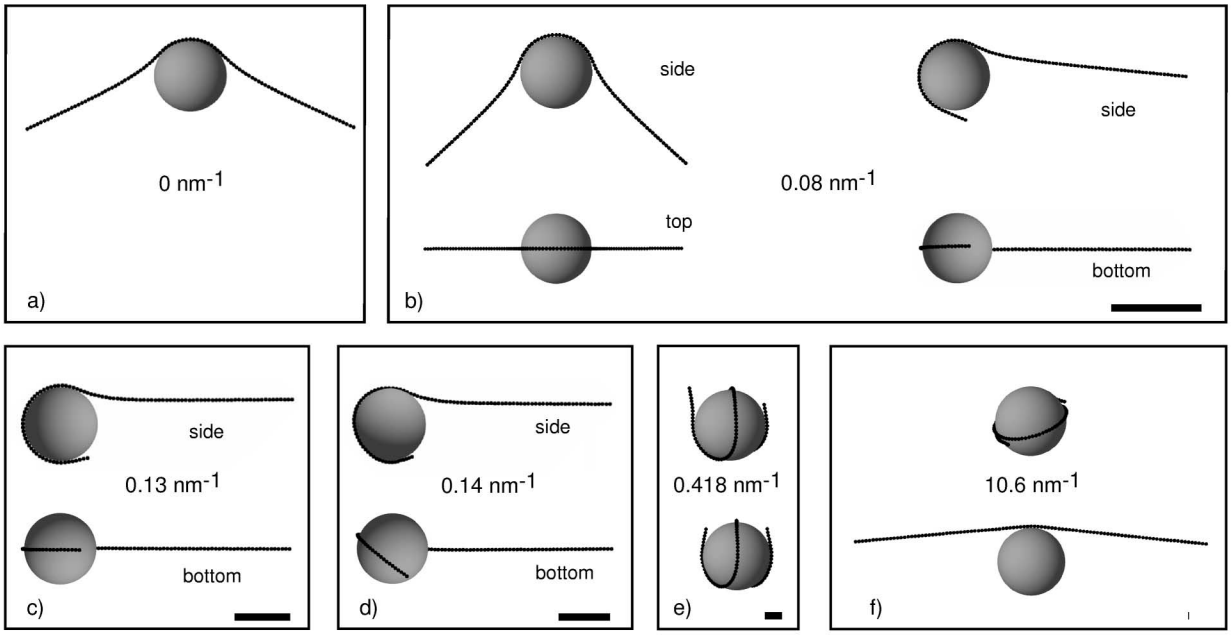

FIG. 1. DNA configurations as obtained by numerical minimization of the free energy (1) for fixed sphere charge $Z = 40$ at increasing salt concentrations. Bars on the lower right indicate the respective screening lengths (except when infinite). (a) No added salt, $\kappa = 0$, the resulting configuration shows rotational symmetry and mirror symmetry. (b) At $\kappa = 0.08$ nm^{-1} (corresponding to a monovalent salt concentration $0.6mM$) the rotational symmetry is discontinuously broken and both structures shown coexist. The polymer is still planar as demonstrated by the top and bottom views. At $\kappa = 0.13$ nm^{-1} ($1.6mM$) the mirror symmetry is continuously broken. (c) Shows the planar configuration right at the transition; (d) shows the nonplanar configuration at a slightly elevated salt concentration $\kappa = 0.14$ nm^{-1}. (e) At $\kappa = 0.418$ nm^{-1} ($16.6mM$) the rotational symmetry is restored in a weakly discontinuous transition, as witnessed by the two coexisting structures which are rather similar. (f) Coexistence between fully wrapped and high-salt-expanded conformation at $\kappa = 10.6$ nm^{-1} ($10.6M$).

complex is strongly overcharged for all $Z < 300$. The dotted line is the high-salt prediction for the wrapping transition obtained from locally balancing the bending energy per unit length $\simeq l_P/2R^2$ with the electrostatic attraction per unit length $\simeq l_B Z\tau/\kappa R^2$ leading to $Z \simeq l_P\kappa/2l_B\tau$ [14]. It agrees well with our numerical results for large salt concentration and also with experimental results for the complexation of PE with charged micelles [2]. Figure 3(b) shows an enlarged view of the low-κ region with all transitions. The bottom line denotes the transition from the fully symmetric state ($\eta = 0, \sigma = 0$) to the rotationally asymmetric state ($\eta \neq 0, \sigma = 0$). This transition is continuous below $Z = 34$ and discontinuous above; the tricritical point is denoted by a square. The middle line is the transition between the rotationally asymmetric state ($\eta \neq 0, \sigma = 0$) and the fully asymmetric state ($\eta \neq 0, \sigma \neq 0$); it is continuous and terminates at a critical end point (denoted by a triangle) at a charge $Z = 55$. Between $Z = 55$ and $Z = 62.5$ there is a direct, discontinuous transition between the fully symmetric ($\eta = 0, \sigma = 0$) and the completely asymmetric state ($\eta \neq 0, \sigma \neq 0$). The upper line is the same line drawn in Fig. 3(a). The three lines do not meet, even at very high salt concentrations. The true histone charge is not known precisely; for $Z \approx 12$, we predict a wrapped (i.e., symmetry-broken) complex for a range of salt concentrations between $4mM$ and $900mM$, close to experimental values for the histone-DNA release thresholds [15]. The broken lines in Fig. 3 denote lines of constant complexation energy of $5k_BT$ and $10k_BT$, where the complexation energy is defined as the difference of the free energy Eq. (1) in the ground state and the reference state consisting of unbent DNA touching the sphere. It

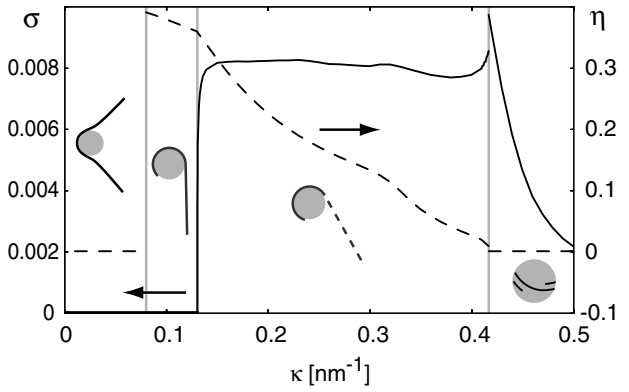

FIG. 2. Rotational order parameter η (dashed line) and torsional order parameter σ (solid line) for fixed sphere charge $Z = 40$ for different salt concentrations. The icons represent all different symmetry states, from left to right: ($\eta = 0, \sigma = 0$), ($\eta \neq 0, \sigma = 0$) , ($\eta \neq 0, \sigma \neq 0$), ($\eta = 0, \sigma \neq 0$).

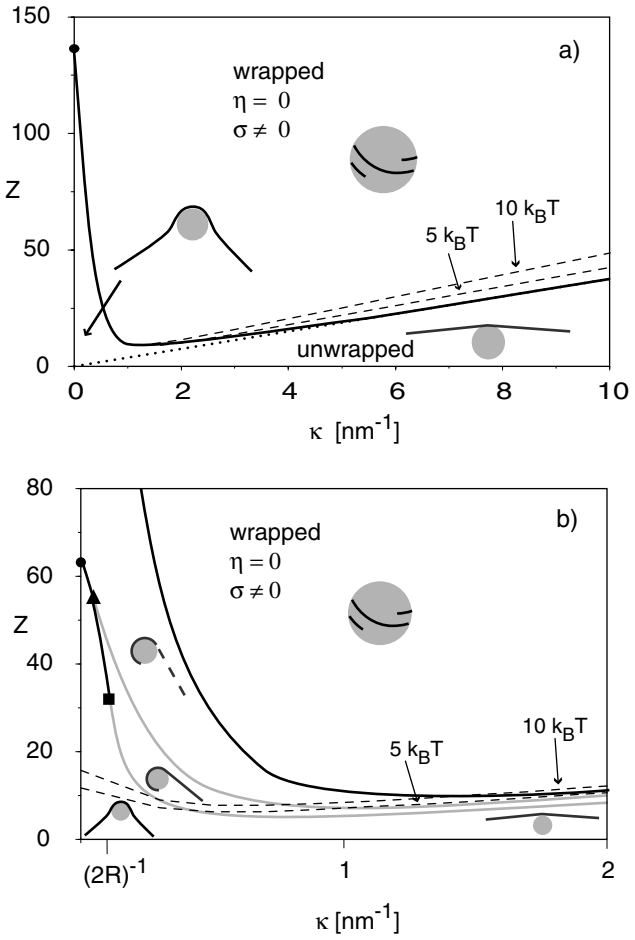

FIG. 3. Phase diagram as a function of sphere charge Z and inverse screening length κ. The dashed lines indicate a complexation energy of 5 and 10 k_BT. (a) The solid line indicates the transition from the rotationally symmetric, mirror-asymmetric state ($\eta = 0, \sigma \neq 0$) to the totally asymmetric state ($\eta \neq 0, \sigma \neq 0$). The minimal sphere charge to wrap the DNA occurs at $\kappa^{-1} \approx 1$ nm corresponding to the physiological condition. The dotted line denotes the high-salt scaling prediction for the wrapping transition (see text). (b) Detail of phase diagram for small κ, featuring all four different phases. Discontinuous (continuous) transitions are denoted by black (gray) solid lines.

is seen that the complexation free energy is much larger than k_BT except very close to the high-salt wrapping transition. This shows that thermally induced dewrapping can be neglected in the main part of the phase diagram.

Extensions to the cases of (i) renormalized DNA charge, (ii) many histones binding to one DNA molecule, (iii) many DNA molecules binding to one histone, and (iv) complexes under externally applied stress are on the way. Our preliminary results indicate that applied forces induce conformational changes and also symmetry-breaking transitions in the range of 1 to 100 pN, well accessible to atomic-force microscopy [21].

Discussions with J. F. Joanny are acknowledged.

[1] G. B. Sukhorukov, E. Donath, S. Davis, H. Lichtenfeld, F. Caruso, V. I. Popov, and H. Möhwald, Polym. Adv. Technol. **9**, 759 (1998).
[2] D. W. McQuigg, J. I. Kaplan, and P. L. Dubin, J. Phys. Chem. **96**, 1973 (1992).
[3] J.Xia, P. L. Dubin, and H. Dautzenberg, Langmuir **9**, 2015 (1993).
[4] F. Ganachaud, A. Elaissari, C. Pichot, A. Laayoun, and P. Cros, Langmuir **13**, 701 (1997).
[5] A. U. Bielinska, J. F. Kukowska-Latallo, and J. R. Baker, Biochim. Biophys. Acta **1353**, 180 (1997).
[6] P. H. von Hippel, D. G. Bear, W. D. Morgan, and J. A. McSwiggen, Annu. Rev. Biochem. **53**, 389 (1984).
[7] T. Wallin and P. Linse, Langmuir **12**, 305 (1996); J. Phys. Chem. **100**, 17 873 (1996); J. Phys. Chem. B **101**, 5506 (1997).
[8] E. M. Mateescu, C. Jeppesen, and P. Pincus, Europhys. Lett. **46**, 493 (1999).
[9] F. von Goeler and M. Muthukumar, J. Chem. Phys. **100**, 7796 (1994).
[10] P. Haronska, T. A. Vilgis, R. Grottenmüller, and M. Schmidt, Macromol. Theory Simul. **7**, 241 (1998).
[11] E. Gurovitch and P. Sens, Phys. Rev. Lett. **82**, 339 (1999).
[12] N. L. Marky and G. S. Manning, J. Mol. Biol. **254**, 50 (1995).
[13] H. Schiessel, J. Rudnick, R. Bruinsma, and W. M. Gelbart, Europhys. Lett. **51**, 237 (2000).
[14] R. R. Netz and J.-F. Joanny, Macromolecules **32**, 9013 (1999); **32**, 9026 (1999).
[15] T. D. Yager, C. T. McMurray, and K. E. van Holde, Biochemistry **28**, 2271 (1989).
[16] E. C. Uberbacher, V. Ramakrishnan, D. E. Olins, and G. J. Bunick, Biochem. **22**, 4916 (1983).
[17] D. W. Brown, L. J. Libertini, and E. W. Small, Biochem. **30**, 5293 (1991).
[18] L. J. Libertini and E. W. Small, Nucl. Acids Res. **15**, 6655 (1987).
[19] The effective persistence length also includes electrostatic contributions, contained in the third term in Eq. (1). At physiological salt concentrations of $0.1M$ this increases l_P to 50 nm; see E. S. Sobel and J. A. Harpst, Biopolymers **31**, 1559 (1991).
[20] M. Fixman, J. Chem. Phys. **76**, 6346 (1982).
[21] M. Rief, H. Clausen-Schaumann, and H. E. Gaub, Nat. Struct. Biol. **6**, 346 (1999).